Int. J. Aquat. Biol. (2025) 13(2): 96-104
ISSN: 2322-5270; P-ISSN: 2383-0956
Journal homepage: www.ij-aquaticbiology.com

Original Article

Structural surface properties of perspective marine antifouling coating based on bimetallic nanoparticles in organic matrix

Andrew A. Mosunov, Yuriy O. Velyaev*[1], Vladislav P. Evstigneev

Sevastopol State University, Universitetskaya St., 33, Sevastopol, 299053, Russia.

Abstract: The paper presents the results of a study on the potential protective anti-fouling coating obtained through the uniform distribution of bimetallic oxide nanoparticles containing copper and iron atoms within an organic matrix. The organic matrix was formed by mixing a suspension of the nanoparticles in xylene with a styrene-acrylic resin. Data on the dynamic light scattering of the initial xylene suspensions and similar suspensions stabilized by centrifugation are provided. The suspension produced an anti-fouling coating, which was investigated using atomic force microscopy and scanning electron microscopy methods. It is demonstrated that as the mass fraction of particles in the matrix increases, noticeable agglomeration occurs. Additionally, exceeding a mass concentration of 20% leads to their uneven distribution within the organic matrix. The results of testing CuO-FeCuO nanoparticles-based antifouling coating in seawater regarding its biocidal effect on heterotrophic bacteria are presented. It is shown that the coating reduces the microfouling effect by 85% compared to an unprotected similar sample.

Article history:
Received 29 November 2024
Accepted 26 January 2025
Available online 25 April 2025

Keywords:
Nanoparticles
SEM
Atomic force microscopy
Polymer matrix
Anti-fouling coating
Agglomeration

Introduction

The biofouling problem on vessels, hydraulic structures, and any surfaces immersed in water has remained highly relevant throughout human engineering advancement over water barriers. Any technical assets designed for use on aquatic entities become subject to biofouling (Macleod et al., 2016; Loxton et al., 2017). The operational costs induced by this phenomenon have led to the development of various methods to resist the attachment of aquatic organisms. Currently, one of the primary methods to counter this issue involves coating the target surface with a special composition containing a significant volume of agents that hinder the growth of living organisms on the treated surface. Copper compounds (primarily their oxide) are among the key active components in contemporary formulations. Despite its effectiveness, research indicates that this substance exerts noticeable adverse effects on "non-target" aquatic organisms (Smirnova and Anninskaya, 2003). Therefore, the task arises to seek new active substances, including those of composite origin (Li et al., 2018; Atacan, 2019; Schorne-Pinto et al., 2019; Liu et al., 2021; Zhang et al., 2021) or approaches that, while comparably effective to current ones, yield fewer side effects.

In collaboration with the Institute of Strength Physics and Materials Science of the Siberian Branch of the Russian Academy of Sciences (SBRAS), it was proposed to employ nanoparticles of various metals and their oxides as such agents (Lerner et al., 2016; Bakina et al., 2019; Svarovskaya et al., 2020). Over the past few years, we have been studying the effectiveness of different compositions containing nanoparticles within a polymer matrix at a marine test site in Sevastopol Bay. This study identified a technical limitation: an increase in nanoparticle concentration led to enhanced agglomeration, resulting in coating non-uniformity and variation in properties from point to point. In standard antifouling coatings, the content of abiotic agents reaches up to 30% without affecting the quality of the resultant surface (Lewis, 2009; Thomas and Brooks, 2010; Covaliu et al., 2011; Dobretsov and Thomason, 2011;

*Correspondence: Yuriy O. Velyaev
E-mail: velyaevyo@yandex.ru

DOI: https://doi.org/10.22034/ijab.v13i2.2377

Inbakandan et al., 2013; Tarrío-Saavedra et al., 2014; Dahms and Dobretsov, 2017; Thakare et al., 2018; Nakanishi et al., 2021). In a parallel yet unpublished experiment, we demonstrated that a 10% concentration does not effectively counter biofouling, indicating the need for further research. Therefore, the research objective was to produce coatings based on CuO-FeCuO nanoparticles within the concentration range of 5 to 30% in an acrylic matrix and to study their structural and surface properties.

Materials and Methods

In our study, the polymer organic matrix was represented by an acrylic resin consisting of Axopol-070 and xylene (GOST 9410-78), used as a solvent. Specific masses of particle loadings were introduced into the solvent and then subjected to dispersion using an ultrasonic disperser model UP200Ht Hielscher. The emitted power was 25 W, and the processing duration was 1 hour. Subsequently, the obtained nanoparticle suspension in xylene was mixed in a 50%/50% ratio with the acrylic resin while continuously stirring. The prepared mixture was then applied to a polymer substrate, and the drying process was conducted at room temperature for 48 hours within an environmentally isolated container. In this manner, six samples were obtained within the 5-30% concentration range at intervals of 5%.

For atomic force microscopy (AFM) data acquisition, the Ntegra Spectra microscope was employed, utilizing a HA_FM/W2C+/50 cantilever (tip radius 35 nm). The force spectroscopy method Fz = Fz(z) of contact mode scanning was used (constant force mode Fz=Fconst≈20 nN). The morphology of the resulting sample was investigated using a Phenom ProX scanning electron microscope (SEM) with an accelerating potential of 5 kV. The EPMA was conducted with the same microscope at an accelerating potential of 15 kV.

Particle size distribution was measured using a Zetasizer Ultra analyzer. For this purpose, an initial nanoparticle solution was prepared with a concentration of 16 mg/mL by loading CuO-FeCuO dry powder into isopropyl alcohol and placing it in a plastic cuvette (1 cm). Then, the solution was diluted as follows: a certain volume (V_{ex}, mL) was first taken from the cuvette, and then a certain volume (V_{in}, mL) of isopropyl alcohol was added. The nanoparticle concentration was determined using the formula: $C_{i+1} = C_i ((V_i-V_{ex}) / (V_i-V_{ex} +V_{in}))$, where V_i stands for the volume of the solution in the cuvette at the i-th step of titration. Hence, nanoparticle concentration was decreasing, and at each concentration level, five measurements of the hydrodynamic diameter of colloidal nanoparticles were performed. Averaging these five values provided the mean hydrodynamic diameter and a measurement error.

Determining dynamic and static friction coefficients for clean and anti-fouling coated samples was conducted using the Labthink MXD-02 Coefficient of Friction Tester. For the measurements, a sample was attached to a specialized weight with a mass of 200 grams. Subsequently, the sample with the attached weight was placed on the measuring platform made of special steel. Before setting the sample on, the measuring platform was also cleaned with ethyl alcohol. On one side, a special transparent polymer thread, which came as part of the instrument's kit, was hooked onto the weight, and on the other side, to the instrument's detector through special holes using terminal hooks. Before initiating the device, the absence of an angle of deviation from the horizontal plane was checked using a built-in level indicator.

The surface acid-base properties of nanoparticles were investigated according to Park's methodology (Parks and de Bruyn, 1962). Potentiometric titration of 0.5 g of CuO-FeCuO was performed, and the results were compared with identical data for a reference sample, which was a 0.1N NaCl solution. Prior to titration, 5 mL of 0.1N NaOH was added to the solution to be titrated. The titration was conducted using 0.1N HCl, with a titrant addition rate of 0.5 mL per minute. The relationship between the specific surface charge and the pH was determined based on the data obtained after titration. Such relationships were obtained for all samples. Hydrogen ion activity was measured using a pH meter, pH-420, with a combined electrode ESLK-01.7, which was immersed

Table 1. Average sizes of nanoparticle clusters depending on the concentration in the coating.

Nanoparticles concentration	5%	10%	15%	20%	25%	30%
By band 100×100 microns						
Average size of nanoparticle clusters, nm	602.937	157.235	268.853	327.020	1072.544	271.607
r.m.s. deviations, nm	77.798	15.644	23.152	29.445	87.105	24.070
By band 10×10 microns						
Average size of nanoparticle clusters, nm	76.880	435.542	177.088	129.622	84.048	111.964
r.m.s. deviations, nm	5.718	73.542	16.211	11.180	7.470	11.951

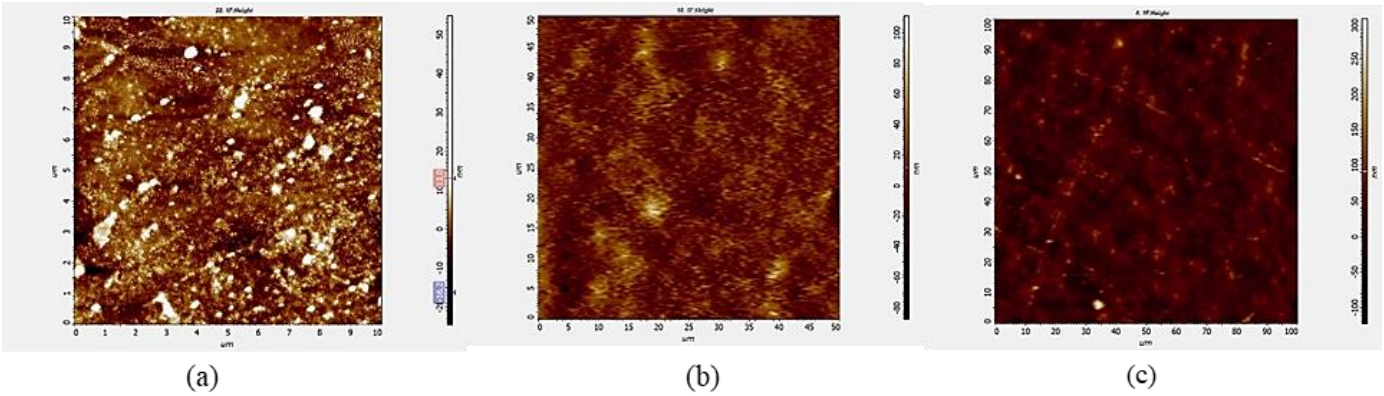

Figure 1. (a) Band 10×10 μm, 5% concentration of nanoparticles CuO-FeCuO, (b) Band 100×100 μm, 10% concentration of nanoparticles CuO-FeCuO, and (c) Band 100×100 μm, 20% concentration of nanoparticles CuO-FeCuO.

in the solution being titrated.

The test for antifouling properties was conducted in Sevastopol Bay, Black Sea. The study used acrylic glass plates (polymethyl methacrylate) with dimensions of 10x15 cm, a thickness of 3 mm, and a surface area of 150 cm², coated with an antifouling layer based on CuO-FeCuO (5 wt. %) and Axpol. As controls, samples without coating and with standard commercial antifouling ship paint, the “Bioplast 52” were used. The samples were installed in a cassette 3 cm apart from each other, perpendicular to the water surface, and submerged to a depth of 2 meters. The experiment lasted for two months, during which the water temperature ranged from 21.8 to 25.5°C.

Fouling microorganisms were analyzed four times during the exposure period of the plates. The dynamics of heterotrophic bacteria populations were studied in the samples. The biofouling film from the surface of the plates coated with the antifouling composition was collected with a cotton swab and placed into pre-prepared test tubes containing sterile seawater (1 ml of water per tube). To determine the number of heterotrophic bacteria, a seeding method was used: 1 ml of the initial suspension was placed in a Petri dish and covered with 10 ml of sterile agar medium, first melted, and then cooled to 45°C. The number of colonies grown was determined on the 4th–5th day after incubation in a thermostat at 27-28°C. The bacterial abundance (CFU) was calculated per 1 cm² of fouled surface using the following formula: $M = (A \times V_1) / (V_2 \times S')$, where M stands for heterotroph abundance in CFU per 1 cm², A is the number of colonies grown on the Petri dish, V_1 is the volume of the initial suspension, and V2 is the volume of the suspension used for seeding, S is the surface area of the investigated object.

Results and Discussions

The AFM data demonstrate a monotonic increase in the average size of nanoparticle clusters in the obtained coatings. Table 1 presents the mean values of nanoparticle cluster sizes measured at 10 points and the corresponding standard deviations of the results. The absence of a specific pattern in the measurements of nanoparticle cluster sizes across the 10×10 μm area could be attributed to the fact that the cantilever tip passed over this area multiple times, causing certain damage. This is related to the sequential reduction in the scanning area as follows: 100×100, 50×50, 30×30, and 10×10 μm. Meanwhile, in measurements over the

Table 2. The ultimate composition of the resulting composite coatings.

Particles concentration in the sample, %	Mass content, %			
	Carbon	Oxygen	Iron	Copper
5	56.18	41.76	2.06	0.00
10	52.56	33.78	3.04	10.62
15	47.00	32.83	3.42	16.75
20	43.11	32.58	3.91	20.39
25	38.43	35.05	5.13	21.39
30	37.41	34.76	5.50	22.33

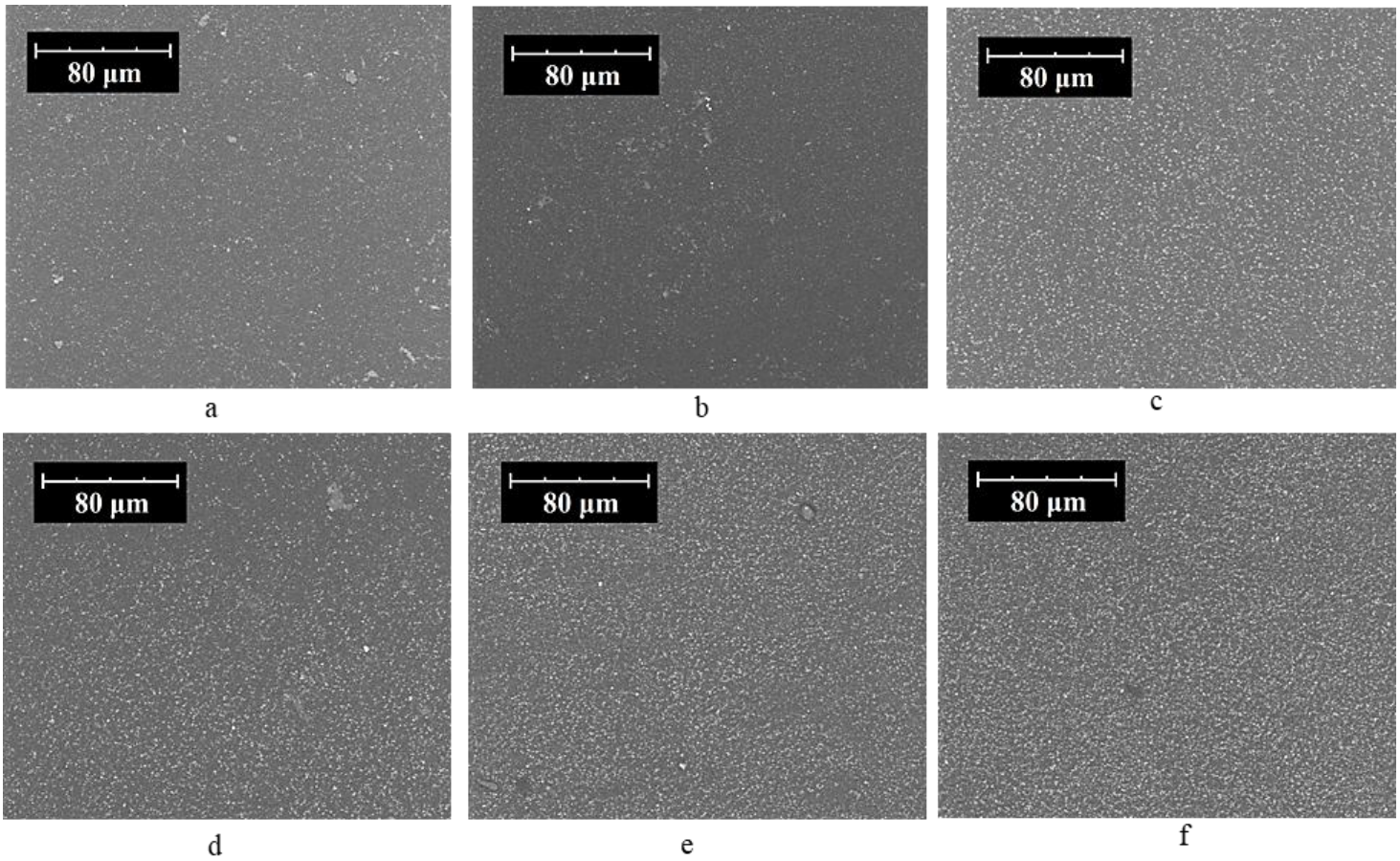

Figure 2. Morphology of the obtained composite coatings, where the mass content of CuO-FeCuO particles corresponds to: (a) 5%; (b) 10%; (c) 15%; (d) 20%; (e) 25%; (f) 30%, (1000X).

100×100 µm area, a monotonic increase in cluster sizes can be observed (except for the lowest and highest concentrations). The reason for the peculiar behavior of these two extreme points is planned to be investigated in further studies. For illustration, several images of the coating obtained by AFM are provided in Figure 1.

The data on the morphology of the obtained coatings are presented in Figure 2. These data clearly show the increase of metallic inclusions in the surface layer of the organic matrix, which correlates well with the AFM data provided in Table 2. Additionally, SEM indicated that with the increase of CuO-FeCuO nanoparticle concentration in the organic matrix, there is a tendency toward intermolecular agglomeration. This leads to forming distinct and significant clusters of these particles on the surface. Notably, such large aggregates begin to appear when concentrations of CuO-FeCuO exceed 20% for coating production.

The results mentioned above have shown that the suspension contains nanoparticles of various sizes, their agglomerates, and "fragments" of microexplosion which is the primary method for obtaining the nanoparticles we used. In light of this, in the next stage of our work, we attempted to achieve maximum homogeneity of nanoparticle suspension.

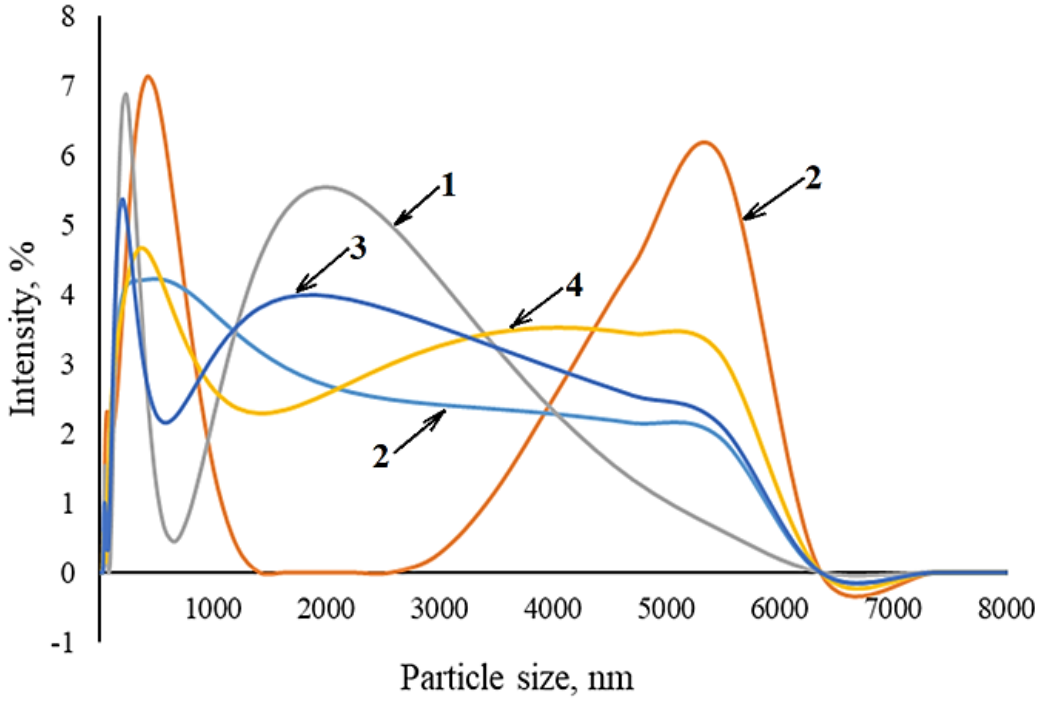

Figure 3. Particle sizes in the initial suspension according to dynamic light scattering data, for solutions with a concentration of bimetallic particles (1 = 5%, 2 = 10%, 3 = 15%, 4 = 20%, and 5 = 25%).

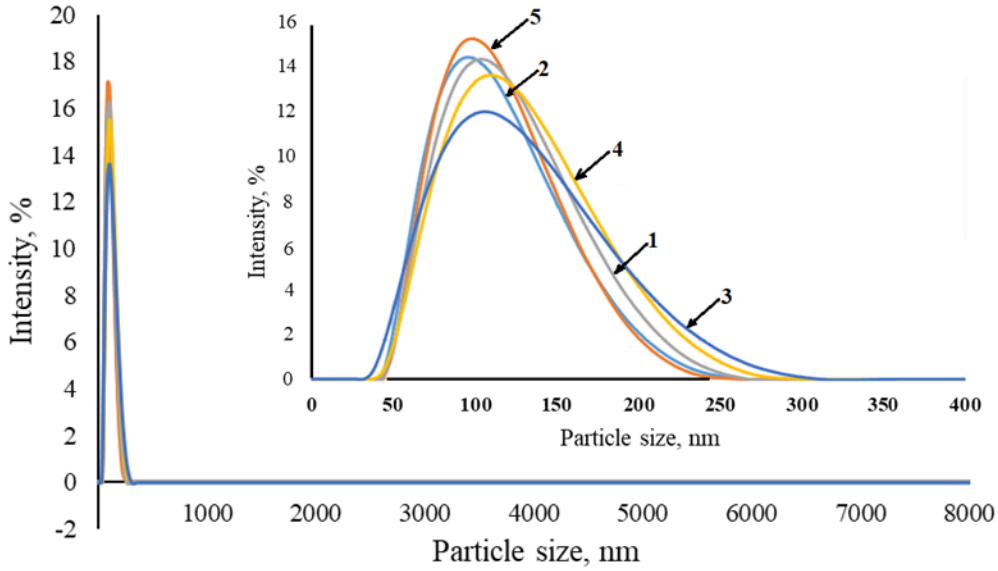

Figure 4. Particle sizes in the initial suspension according to dynamic light scattering data (on the insert, the peak area is expanded), for solutions with a concentration of bimetallic particles (1 = 5%, 2 = 10%, 3 = 15%, 4 = 20%, and 5 = 25%).

To do this, we took the particle sample and placed it in isopropyl alcohol to attain different weight concentrations within the previously specified range. We did not investigate a weight concentration of 30% because it resulted in a sufficiently viscous and challenging-to-mix suspension. We processed the obtained suspensions using an ultrasonic disperser following the methodology described earlier. To control the size distribution of the obtained particles, we employed a Zetasizer Ultra particle analyzer. Particle size distribution by the intensity of the scattered light is shown in Figure 3. The curve analysis shows that the suspension contains particles with sizes spanning a broad size range.

To achieve greater homogeneity, we subjected the suspension to centrifugation using a Liston C 2204

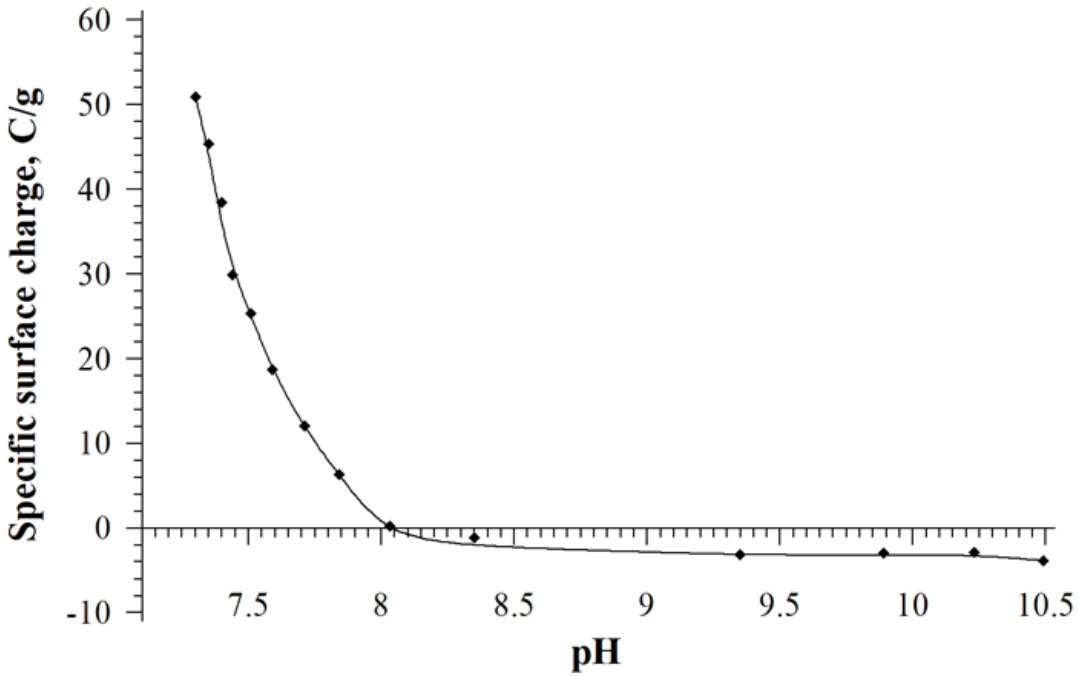

Figure 5. Distribution of specific surface charge for CuO-FeCuO particles.

centrifuge at a rotational speed of 3000 rpm for 20 minutes. As a result, a homogeneous suspension of particles with an average dynamic particle radius in the mixture of 97.26 nm was obtained (Figure 4). The results of this stage enable us to conclude that centrifugation of the initial solution significantly improves its quality in terms of particle sizes. However, this method has a significant drawback - losing up to 99% of the initial nanoparticle load after centrifugation. On the other hand, if an antifouling coating mixture is prepared without prior centrifugation and separation of large fractions, a certain increase in surface roughness is observed. This increased roughness can suppress marine microorganisms but, at the same time, mechanically represents a more likely environment for adhesion to the surface. As a result, standard coatings were obtained using this approach, and dynamic and static friction coefficients were measured for the plate without coating (0.141 and 0.132) and with the coating (0.154 and 0.144), respectively. These measurements showed that applying a coating to the sample obtained without additional deagglomeration increases friction coefficients by 9%, which correlates with the AFM data presented earlier. Therefore, coatings obtained this way will be effective against microorganisms that cause microfouling, but it is unlikely to reduce macrofouling due to the increased surface roughness.

Indeed, the agglomeration of particles is a significant drawback. This phenomenon can be attributed to accumulated surface electrostatic charge, which leads to their subsequent aggregation. The extent of agglomeration is largely dependent on the medium in which these particles are suspended. In our study, a non-aqueous base, namely an organic solvent, was used, so we cannot speak about its pH value, which could be measured in the case of aqueous solutions. However, understanding the distribution of the specific surface charge of the nanoparticles used in our research may be helpful when preparing coatings in aqueous-based systems. In such systems, much less agglomeration of nanoparticles and, consequently, greater coating efficiency may be achieved.

The pH value is a crucial factor for aqueous solutions. The pH value at which the surface charge density of suspended particles equals zero is known as the point of zero charge (pH_{zcp}) for a particular substance. At this pH level, minimal interaction with the solvent occurs, making deagglomeration by applying ultrasound more effective. Furthermore,

Table 3. The number of heterotrophic microorganisms on the plates depending on the exposure time.

Plate coating	Heterotrophic abundance after *n* days of exposure, 10^2 CFU/cm^2			
	n=3	*n*=14	*n*=21	*n*=56
Without coating	0.73	1.77	2.58	3.96
Bioplast 52	0.11	0.16	1.21	3.21
CuO-FeCuO + Axopol-070	0.40	1.13	0.91	0.61

reverse aggregation in the case of equidistant particles, is almost negligible.

In this study, the pH_{zcp} for this type of nanoparticle was determined and presented in Figure 5. For this particle type, pH_{zcp} = 8.075 indicates that interactions with the solvent are minimized at this pH value. Using water-based paints with adjustable pH levels can reduce particle agglomeration, especially at relatively high particle concentrations (Fig. 5). This, in turn, could enhance the anti-fouling effectiveness of coatings prepared using such paint.

To achieve a concentration of nanoparticles that can potentially exhibit a noticeable anti-fouling effect, one shall use concentrations of the active agent (nanoparticles) in the range of 10 to 20% by mass or modify the coating fabrication protocol. Another approach could be switching to water-based paint, in which the pH of the medium can be adjusted to mitigate electrostatic interactions between particles, leading to their agglomeration. Even a slight shift in the pH of the medium to a weakly alkaline range, up to a value of 8.075, can compensate for the surface charge of the studied particles and, as a result, potentially enhance their deagglomeration within the framework of the standard coating fabrication protocol. However, despite an agglomerating factor, this biocide should still exhibit high efficacy in traditional paint formulations, which needed to be verified experimentally.

The antifouling efficacy of the composition presented in the study was assessed, with the data shown in Table 3 demonstrating its effectiveness as a biocide. The uncoated plate exhibited a gradual increase in the number of fouling microorganisms. The commercial antifouling paint significantly reduced the growth rate of heterotrophs, leading to a 17% decrease in the overall mass of fouling organisms. Meanwhile, although the CuO-FeCuO biocide under study showed slightly worse results than the commercial paint during the first two weeks, it demonstrated greater effectiveness over a longer period, achieving an 85% reduction in microfouling compared to the control sample without coating.

Conclusions

In this study, we examined some of the physicochemical properties of the biocide that were proposed as the main active component for creating an effective antifouling coating for marine vessels. Using SEM and AFM, we studied the morphology of the proposed coatings as a function of the mass concentration of CuO-FeCuO bimetallic nanoparticles in it (in concentrations ranging from 5 to 30%) mixed with Axpol in the aforementioned mass ratios. A directly proportional relationship was observed between the agglomeration process of nanoparticles and their mass fraction in the coating. This is likely due to their electrostatic interactions, resulting from the nanoparticles' accumulation of specific surface charge, which was also investigated. Indeed, particle agglomeration increases the friction coefficient for objects with the coating, which may serve as an additional factor aiding microorganisms in adhering to the outer surface, as demonstrated by the field exposure experiment. However, over time, the biocide's effect yields results: unlike other coatings or in their absence, the population of microorganisms, exemplified by heterotrophs, does not increase but rather decreases. This was likely due to the toxic action of the biocide. Consequently, it can be assumed that the absence or reduced growth of the initial microbiological film will slow down the subsequent fouling by larger hydrobionts that feed on the primary bacterial environment, thereby achieving the desired antifouling effect of the proposed coating.

Acknowledgements

The equipment for the study was provided by of Shared Research Facilities “Center for Perspective Technologies and Materials” of Sevastopol State University.

References

Atacan K. (2019). $CuFe_2O_4$/reduced graphene oxide nanocomposite decorated with gold nanoparticles as a new electrochemical sensor material for Ï-cysteine detection. Journal of Alloys and Compounds, 791: 391-401.

Bakina O.V., Glazkova E.A., Svarovskaya N.V., Rodkevich N.G., Lerner M.I. (2019). «Janus»-like Cu-Fe bimetallic nanoparticles with high antibacterial activity. Materials Letters, 242: 187-190.

Covaliu I.C., Neamtu J., Georgescu G., Malaeru T., Cristea C., Jitaru I. (2011). Synthesis and characterization of ferrites (Fe_3O_4/$CuFe_2O_4$)-calcium alginate hybrids for magnetic resonance imaging. Digest Journal of Nanomaterials and Biostructures, 6(1): 245.

Dahms H.U., Dobretsov S. (2017). Antifouling compounds from marine macroalgae. Marine Drugs, 15(9): 265.

Dobretsov S., Thomason J.C. (2011). The development of marine biofilms on two commercial non-biocidal coatings: A comparison between silicone and fluoropolymer technologies. Biofouling, 27(8): 869-880.

Inbakandan D., Kumar C., Abraham L., Kirubagaran R., Venkatesan R., Khan S. (2013). Silver nanoparticles with anti microfouling effect: a study against marine biofilm forming bacteria. Colloids and Surfaces B: Biointerfaces, 111: 636-643.

Lerner M.I., Pervikov A.V., Glazkova E.A., Svarovskaya N.V., Lozhkomoev A.S., Psakhie S.G. (2016). Structures of binary metallic nanoparticles produced by electrical explosion of two wires from immiscible elements. Powder Technology, 288: 371-378.

Lewis J.A. (2009). Non-silicone biocide-free antifouling solutions. In: Woodhead Publishing Series in Metals and Surface Engineering, Advances in Marine Antifouling Coatings and Technologies, 709-724.

Li Q., Yong C., Cao W., Wang X., Wang L., Zhou J., Xing X. (2018). Fabrication of charge reversible graphene oxide-based nanocomposite with multiple antibacterial modes and magnetic recyclability. Journal of Colloid and Interface Science, 511: 285-295.

Liu J.M., Lu Y.H., Xu Z.F., Wang R.X., Yan H.C., Li X. (2021). Effect of citric acid-to-nitrate ratio on combustion synthesis of $CuFe_2O_4$ for sodium-ion storage. Journal of Materials Science: Materials in Electronics, 32: 94-101.

Loxton J., MaCleod A.K., Nall C.R., McCollin T., Machado I., Simas T., Vance T., Kenny C., Want A., Mille R.G. (2017). Setting and agenda for biofouling research for marine renewable energy industry. International Journal of Marine Energy, 19: 292-303.

Macleod A., Stanley M., Day J., Cook E. (2016). Biofouling community composition across a range of environmental conditions and geographical locations suitable for floating marine renewable energy generation. Biofouling, 32(3): 261-276.

Nakanishi E.Y., Palacios J.H., Godbout S., Fournel S. (2021). Interaction between biofilm formation, surface material and cleanability considering different materials used in pig facilities – an overview. *Sustainability,* 13: 5836.

Parks G.A., de Bruyn P.L. (1962). The zero point of charge of oxides. The Journal of Physical Chemistry, 66: 967-973.

Schorne-Pinto J., Cassayre L., Presmanes L., Barnabé A. (2019). Insights on the stability and cationic nonstoichiometry of $CuFeO_2$ delafossite. Inorganic Chemistry, 58: 6431-6444.

Smirnova L.L., Anninskaya I.N. (2003). Distribution of copper compounds in the marine environment and bottom sediments of port waters. Environmental Safety of Coastal and Shelf Zones, 9: 106. (in Russian)

Svarovskaya N.V., Bakina O.V., Pervikov A.V., Rubtsov K.V., Lerner M.I. (2020). Electrical explosion of wires for manufacturing bimetallic antibacterial Ti-Ag and Fe-Ag nanoparticles. Russian Physics Journal, 62: 1580-1586.

Tarrío-Saavedra J., López-Beceiro J., Naya S., Francisco-

Fernández M., Artiaga R. (2014). Simulation study for generalized logistic function in thermal data modeling. Journal of Thermal Analysis and Calorimetry, 118: 1253-1268.

Thakare P.S., Padole P.R., Bodade A.B., Chaudhari G.N. (2018). Microstructural and antifungal properties of silver substituted copper ferrite nanopowder synthesized by sol-gel method. Indo American Journal of Pharmaceutical Sciences, 5: 52-63.

Thomas K.V., Brooks S. (2010). The environmental fate and effects of antifouling paint biocides. Biofouling, 26(1): 73-88.

Zhang Y., Chen Y., Kang Z.V., Gao X., Zeng X., Liu M., Yang D.P. (2021). Waste eggshell membrane-assisted synthesis of magnetic $CuFe_2O_4$ nanomaterials with multifunctional properties (adsorptive, catalytic, antibacterial) for water remediation. Colloids and Surfaces A: Physicochemical and Engineering Aspects, 612: 125874.